

## Article

# Conterminous United States Land-Cover Change (1985–2016): New Insights from Annual Time Series

Roger F. Auch <sup>1,\*</sup>, Danika F. Wellington <sup>2</sup>, Janis L. Taylor <sup>2</sup>, Stephen V. Stehman <sup>3</sup>, Heather J. Tollerud <sup>1</sup>, Jesslyn F. Brown <sup>1</sup> , Thomas R. Loveland <sup>1</sup>, Bruce W. Pengra <sup>2</sup>, Josephine A. Horton <sup>4</sup> , Zhe Zhu <sup>5</sup>, Alemayehu A. Midekisa <sup>2</sup>, Kristi L. Saylor <sup>1</sup> , George Xian <sup>1</sup>, Christopher P. Barber <sup>1</sup> and Ryan R. Reker <sup>2</sup>

<sup>1</sup> U.S. Geological Survey (USGS), Earth Resources Observation and Science (EROS) Center, 47914 252nd Street, Sioux Falls, SD 57198, USA; htollerud@usgs.gov (H.J.T.); jfbrown@usgs.gov (J.F.B.); loveland@usgs.gov (T.R.L.); sayler@usgs.gov (K.L.S.); xian@usgs.gov (G.X.); cbarber@usgs.gov (C.P.B.)

<sup>2</sup> KBR, Contractor to the U.S. Geological Survey, Earth Resources Observation and Science (EROS) Center, 47914 252nd Street, Sioux Falls, SD 57198, USA; dwellington@contractor.usgs.gov (D.F.W.); jltaylor@contractor.usgs.gov (J.L.T.); bpengra@contractor.usgs.gov (B.W.P.); alemayehu.midekisa@noaa.gov (A.A.M.); rreker@contractor.usgs.gov (R.R.R.)

<sup>3</sup> Department of Forest and Natural Resource Management, State University of New York, Syracuse, NY 13210, USA; svstehman@esf.edu

<sup>4</sup> Innovate! Inc., Contractor to the U.S. Geological Survey, Earth Resources Observation and Science (EROS) Center, 47914 252nd Street, Sioux Falls, SD 57198, USA; jahorton@contractor.usgs.gov

<sup>5</sup> Department of Natural Resources and the Environment, University of Connecticut, Storrs, CT 06269, USA; zhe@uconn.edu

\* Correspondence: auch@usgs.gov; Tel.: +1-605-594-6086



**Citation:** Auch, R.F.; Wellington, D.F.; Taylor, J.L.; Stehman, S.V.; Tollerud, H.J.; Brown, J.F.; Loveland, T.R.; Pengra, B.W.; Horton, J.A.; Zhu, Z.; et al. Conterminous United States Land-Cover Change (1985–2016): New Insights from Annual Time Series. *Land* **2022**, *11*, 298. <https://doi.org/10.3390/land11020298>

Academic Editor: Adrianos Retalis

Received: 7 January 2022

Accepted: 10 February 2022

Published: 16 February 2022

**Publisher's Note:** MDPI stays neutral with regard to jurisdictional claims in published maps and institutional affiliations.

**Abstract:** Sample-based estimates augmented by complete coverage land-cover maps were used to estimate area and describe patterns of annual land-cover change across the conterminous United States (CONUS) between 1985 and 2016. Most of the CONUS land cover remained stable in terms of net class change over this time, but a substantial gross change dynamic was captured by the annual and cumulative time intervals. The dominant types of changes can be grouped into natural resource cycles, increases in urbanization, and surface-water dynamics. The annual estimates over the 30-year time series showed a reduction in the rate of urban expansion after 2006, new growth in cropland after 2007, but a net overall decline in cropland since 1985, and two eras of net tree cover loss, the first one early in the time series and the second starting in 2012. Our study provides a holistic assessment of the CONUS land-cover conversion (class) change and can serve as a new benchmark for future research.

**Keywords:** U.S. land-cover change; natural resource cycles; urbanization; surface-water dynamics



**Copyright:** © The authors are employees of U.S. Geological Survey (USGS), and the article is a U.S. Government Work, published by MDPI, Basel, Switzerland, with the permission of USGS. Licensee MDPI, Basel, Switzerland. This article is an open access article distributed under the terms and conditions of the Creative Commons Attribution (CC BY) license (<https://creativecommons.org/licenses/by/4.0/>).

## 1. Introduction

Land-cover change has been linked with environmental issues at various scales, such as land degradation, changes in biodiversity, intensification of climate change at a global perspective [1,2], increased sedimentation of stream courses, changed land-atmospheric interaction patterns that may alter weather and climatic variability, and carbon balances at regional scales [3]. Local effects include declining water quality in urbanizing areas [4] and diminished ecosystem services from increased agriculture [5]. However, positive effects of such change are also apparent. Afforestation can help slow or reverse decreased ecosystem services by increasing carbon stocks and protecting water supply sources [6,7]. Grass dominated vegetated buffers also have the capacity to slow agricultural and urban nutrient runoff into streams [8,9].

The United States has a land-use system that has matured during the past 400 years. Land-use patterns tracked since World War II have shown little overall change in composition [10], but modernized methods for land-cover monitoring [11] can reveal a far more

complicated change story. Land cover can be used as a surrogate for better understanding land use because optical sensors on numerous satellites measure how light is reflected from what is on the Earth's surface as land cover, although some land-cover classifications can be a mix of both land cover and land use [12]. Remote-sensing scientists have advocated for a comprehensive and sustained terrestrial monitoring program [1,13,14], and this has been echoed by the growing land-change science community. The opening of the Landsat archive to free access [15,16] enabled capturing land surface dynamics at relatively fine temporal scales [17,18]. Enhanced temporal-scale monitoring allows for a better dissection of even generally stable land-use systems.

Multiple land-cover monitoring studies, usually remote sensing based, have focused on a limited set of land-cover classes e.g., [19–21], topical and regional views e.g., [22,23], topical and limited temporal assessments e.g., [24,25], or various combinations thereof e.g., [26]. Some recent studies have generated annual land-cover change analysis but are still limited to a specific topic, such as increases in impervious surfaces (developed land-cover class) at global and national scales [27,28]. Several agencies within the U.S. Department of Agriculture have studies comparable with the spatial and temporal extent used in this study [10,29] that rival this study's spatiotemporal extent, but they concentrate on land use instead of land cover, and thus do not account for the largest land-cover changes found when analyzing U.S. Geological Survey (USGS) land-cover class change mapping efforts: tree cover loss and tree cover gain [1], this study. The long temporal span of this study allows greater ability to discern multiple directions in land-cover conversion that include change across shorter time spans, reciprocal class change that represents the back-and-forth transition between two land covers, and other types of complex land-cover transitions. A prime example is our estimated overall decrease in cropland versus studies that show expanding U.S. cropland during a subset of our study's years e.g., [26,30]. Recently, Radwan et al. [31] showed how at the global and continental scales the major land covers all had gains and losses over time except for "urbanization" that was unidirectional. We build on this discussion of gross land cover change but for the conterminous United States (the 48 physically joined states and the District of Columbia or CONUS) and extend the analysis to include a full set of land-cover classes monitored over a 30+ year period along with examples of drivers affecting such change. This is the first study to generate statistically backed area estimates of total land-cover change for the CONUS on an annual basis between 1985 and 2016.

The dynamics of land cover are complex and become more so as the time dimension increases. One land-cover class conversion (e.g., from tree cover to cropland) is relatively easy to describe, but multiple changes over time can become challenging to track and understand. We discuss "gross change", a year-to-year accounting of all land-cover change, and "net change", the difference between gross change gains and losses. Both gross and net change describe land-cover conversions between two points of time. Certain change processes may be cyclic, where the same location changes multiple times, such as tree cover to grass/shrub and back to tree cover or cropland to grass/shrub and then back to cropland. These linked reciprocal gross changes can result in no net change at that location depending on the two dates used. Thus, over a greater span of time, gross change dynamics and their effects potentially can be underestimated if only net change is tracked between widely separated start and end dates of a study period. The same issue can arise with grouped multi-year intervals where multiple changes can occur at the same location, but change is missed (e.g., fast-growing forestry land use) if the temporal mapping interval is not sufficiently dense. Higher frequency land-cover information contributes to the better understanding of land cover dynamics.

To explore these land-cover change complexities and generate statistically based area estimates of various land-cover class change metrics between 1985 and 2016, we used a sample-based approach on an annual basis. These metrics have been used by others e.g., [32,33]. We also used complete coverage maps to show and describe the spatial distribution of land-cover conversions. From the sample data, we also estimated the area of

the footprint of change (i.e., at least one class change occurred during the time monitored and the area distribution of frequency of class change (e.g., the area that changed once or more during the period)). The sampling and map data are all part of the USGS Land Change Monitoring, Assessment, and Projection (LCMAP) project [11]. The eight land-cover classes included in LCMAP are developed, cropland, grass/shrub, tree cover, water, wetland, ice/snow, and barren (see Appendix A Table A1 for class definitions).

## 2. Materials and Methods

The data used in this study included the sample reference data and 2 of the 10 map products created by the LCMAP project. The reference sample dataset was based on a simple random sample of 24,971 Landsat-resolution ( $30 \times 30$  m) gridded plot areas selected within the LCMAP CONUS map extent. The annual reference class labels were obtained by analysts who interpreted Landsat imagery, high-resolution aerial photography, and other ancillary datasets [34] implemented within a specially developed version of the TimeSync reference data collection tool [35]. Analysts determined multiple attributes of each sampled plot, with the analysts operating under a formal quality assurance/quality control protocol to enhance accuracy and consistency of attribute values [34]. Each sample plot has multiple attributes for each year that were binned into three categories: land use, land cover, and change process, with the absence of change being recorded as stable for a change process. The plot land use and land cover for each year were “cross walked” to a single land-cover class from the eight classes found in the LCMAP primary land cover map product. Because multiple interpreters collected the reference data, a random subsample of plots was selected for an independent (i.e., different analyst) second interpretation to quantify between interpreter consistency. This allowed the generation of approximate accuracy measures of the reference land cover classification and its various changes [34].

The two LCMAP map products used were the annual primary land cover (LCPRI) and the annual land cover-class change (LCACHG) [11]. Each pixel within the annual LCPRI land-cover product has a class code that was assigned based on the CCDC (Continuous Change Detection and Classification) algorithm prediction for the July 1st date of that year [11,17]. This algorithm has lineage back to the Google Earth Engine platform [17] but was refined by the USGS [11,18] to be an operational mapping system. The annual land-cover class change product (LCACHG) has a code for each pixel that represents the land-cover change that has taken place since the previous year. In the same way as the LCPRI product, LCACHG is annualized on the July 1st date, such that any reported change represents the difference between successive LCPRI products. The change is reported in the year in which it is first recognized; thus, the LCACHG product for 1986 indicates class change over the preceding year, or the difference between the 1985 and 1986 LCPRI products. These LCMAP product values were extracted for the plots corresponding to the reference sample locations. Data files containing these values are available online [36], and the results for an accuracy assessment of LCPRI and LCACHG are reported in [37].

Good practice guidance emphasizes that the reference dataset should be the basis for estimates of area of land cover and land-cover change [38]. Considering this, the tables and graphs of area estimates in this work were produced from the reference dataset, with the map products used to reduce standard errors by providing strata for post-stratified estimation of some population parameters.

### *Sample-Based Estimators*

The estimator for the proportion ( $\hat{p}$ ) of area of any change class  $k$  was simply the proportion of sample plots that had the change class as its reference label,

$$\hat{p}_k = \frac{n_k}{n} \quad (1)$$

where  $n_k$  is the number of sample counts in reference class  $k$  and  $n = 24,971$  is the total size of the sample. The standard error (SE) was estimated using

$$SE(\hat{p}_k) = \sqrt{\frac{\hat{p}_k(1 - \hat{p}_k)}{(n - 1)}} \quad (2)$$

To estimate the area of the change class, the estimated proportion of area was multiplied by the CONUS area, and the standard error of the area estimate was produced by multiplying the CONUS area by the standard error of the estimated proportion. The above formulas were also used to produce **area estimates for individual frequencies of land-cover change** (i.e., the estimated area that experienced a specific number of changes over the time span 1985–2016).

To estimate the **area of 1985–2016 net land-cover change** for each sample plot we defined  $y_u$  in square kilometers (1 plot = 0.0009 km<sup>2</sup>) based on the land cover class in 1985 and the land cover class in 2016 as follows:

$$y_u = \begin{cases} +0.0009 & \text{if sample plot } u \text{ changed to the target class (gross gain)} \\ 0 & \text{if sample plot } u \text{ did not change or was not the target class} \\ -0.0009 & \text{if sample plot } u \text{ changed from the target class (gross gain)} \end{cases} \quad (3)$$

Let  $\bar{y}$  be the sample mean of the  $y_u$  values,  $n = 24,971$  is the sample size, and  $N = 8,966,643,894$  is the population size (the total number of pixels in LCMAP's CONUS extent). Then, the estimated area of net change ( $\hat{A}$ ) for a particular land cover class is  $\hat{A} = N\bar{y}$ . The sample variance,  $s^2$ , and standard error of the area estimate are as follows:

$$s^2 = \sum_{u=1}^n \frac{(y_u - \bar{y})^2}{(n - 1)} \quad (4)$$

$$SE(\hat{A}) = Ns/\sqrt{n} \quad (5)$$

Net change at an annual time-step was similarly estimated using the above Equation (3) but defining the start and end dates to be one year different in time for each annual step.

For the **estimated sum of annual gross change over all years**, we defined  $y_u$  in square kilometers for each pixel based on the land-cover class conversions present throughout the time series (1985–2016) as follows:

$$y_u = 0.0009 \times (\text{number of target land cover conversions}) \quad (6)$$

The estimated area and standard error can then be calculated using the same formulas as for net land-cover class change above. The **overall gross change** (total gross change of any type) was estimated by allowing the target land-cover conversion to be any conversion; otherwise, it corresponded to either individual or groups of conversions (such as loss to any other class) as noted.

To estimate the standard error of the **ratio of the area of a specific grouping of class change types** relative to the total area of change (i.e., total area of change for group/total area of change), we defined  $y_u$  and  $x_u$  for each sample plot as shown below, where 0.0009 km<sup>2</sup> is the area of each plot,  $c$  indicates the number of times the plot had the change of the target change group being estimated, and  $d$  indicates the number of times the plot had a change of any kind:

$$y_u = 0.0009 \times c \quad (7)$$

$$x_u = 0.0009 \times d \quad (8)$$

The population parameter of interest is the ratio  $R = \frac{Y}{X}$ , where  $Y$  is the population total of  $y_u$  (total area of class change of the target change group) and  $X$  is the population total of  $x_u$  (total area of all class change). The sample-based estimator of this ratio is

$$\hat{R} = \frac{\hat{Y}}{\hat{X}} = \frac{\bar{y}}{\bar{x}} \quad (9)$$

where  $\bar{x}$  is the sample mean of  $x_u$  and  $\bar{y}$  is the sample mean of  $y_u$ . The estimated variance ( $\hat{V}$ ) of the ratio estimator is (eqn. 6.13 of [39])

$$\hat{V}(\hat{R}) = \left( \frac{1}{n\bar{x}^2} \right) (s_y^2 + \hat{R}^2 s_x^2 - 2\hat{R}s_{yx}) \quad (10)$$

where  $n$  is the sample size,  $s_y^2$  and  $s_x^2$  are the sample variances for  $y_u$  and  $x_u$ , and  $s_{yx}$  is the sample covariance of  $y_u$  and  $x_u$ ,

$$s_{yx} = \frac{1}{n-1} \left[ \sum_{u=1}^n x_u y_u - n\bar{x}\bar{y} \right] \quad (11)$$

The standard error of the estimated ratio is the square root of the estimated variance,  $SE(\hat{R}) = \sqrt{\hat{V}(\hat{R})}$ .

For some estimates, map information was incorporated via post-stratified estimation, where the complete coverage information in the annual time series map products was used to reduce the standard errors of the sample-based area estimates [40]. The post-stratified estimator [38] of the proportion of area of reference class  $k$  is

$$\hat{p}_k = \sum_{i=1}^q W_i \frac{n_{ik}}{n_i} \quad (12)$$

and the standard error of the estimated proportion is:

$$SE(\hat{p}_k) = \sqrt{\sum_i \frac{W_i \hat{p}_{ik} - \hat{p}_{ik}^2}{n_i - 1}} \quad (13)$$

where  $q$  is the number of strata,  $W_i$  is the proportion of area mapped as class  $i$ ,  $n_{ik}$  is the number of sample plots corresponding to map class  $i$  and reference class  $k$ ,  $n_i$  is the sum of the map counts of class  $i$  (i.e., sample size in stratum  $i$ ) and  $\hat{p}_{ik} = n_{ik}/n_i$  is the estimated proportion of the area of reference class  $k$  in map stratum  $i$ . The post-stratified estimator was used to estimate **annual area of land cover (i.e., land-cover composition)** and **annual percent area of change**, as well as the **overall footprint of land-cover change**. For estimating land-cover composition, the annual map land-cover classes were used as strata. For estimating the percent of area of change, the map binary change/no-change categories were used as strata. The two strata for the post-stratified estimator of the overall footprint of change included one stratum defined as all map pixels that have a mapped change for any year in the time series (i.e., the total map footprint of change) and the other stratum defined as all other pixels (i.e., stable pixels with no change in any year of the times series). Post-stratified estimation was not used for annual area of change because of inadequate map accuracy [37], and because some change classes are so rare that very few or even no sample plots were found in the map stratum for that change class.

### 3. Results

#### 3.1. U.S. Land-Cover Change over Three Decades

Based on our estimates of net change, land-cover class composition remained mostly stable between 1985 and 2016 at the CONUS scale (Supplementary Dataset S1). The largest net change was an increase in developed land of  $131,209 \pm 6866 \text{ km}^2$  representing  $1.63\% \pm 0.09\%$  of CONUS area (values to the right of the  $\pm$  are one standard error, SE), followed by a decrease in cropland of  $-109,233 \pm 9485 \text{ km}^2$  representing  $1.35 \pm 0.12\%$  of CONUS area, and a decrease in tree cover of  $-44,921 \pm 9878 \text{ km}^2$  representing  $0.56 \pm 0.12\%$  of CONUS. (Table 1). These, and other changes, occurred over an estimated  $11.5\% \pm 0.18\%$  of CONUS, which represent a footprint of change area of  $927,806 \pm 14,607 \text{ km}^2$  (Table 2) with about 40% of this footprint experiencing change more than once (Table 2). The estimated area of annual gross change summing across all years was  $1,408,393 \pm 28,527 \text{ km}^2$  (Table 3), demonstrating that the relatively small net changes in land-cover composition can involve larger amounts of gross change that come from cumulative annual change. The annual mean rate of gross change was about 0.6% (Figure 1; main part of Table 3) with a standard deviation of the annual rates of 0.1%. The highest rates of change occurred in 1989, 1999, and 2000, and the lowest rates occurred in 1986, 2015, and 2016 (Figure 1). The estimated annual amounts of the leading types of changes influence the overall annual rate of class change, and these types of conversions and some of their approximate drivers are presented in the following sections.

**Table 1.** CONUS land-cover estimated area and net percent change between 1985 and 2016.

Land Cover	Area (km <sup>2</sup> )	SE (km <sup>2</sup> )	Area (%)	SE (%)
Developed	131,209	6866	1.63	0.09
Cropland	-109,233	9485	-1.35	0.12
Grass/Shrub	11,311	12,479	0.14	0.15
Tree Cover	-44,921	9878	-0.56	0.12
Water	7756	3166	0.10	0.04
Wetland	970	2685	0.01	0.03
Ice/Snow	0	0	0.00	0.00
Barren	2909	1409	0.04	0.02

**Table 2.** Estimated area footprint of change and area of individual change frequencies based on the reference dataset (frequency of 0 represents the no-change footprint and frequency of 1+ represents the change footprint).

Change Frequency	Area (%)	SE (%)	Area (km <sup>2</sup> )	SE (km <sup>2</sup> )
0	88.50	0.18	7,142,174	14,607
1+	11.50	0.18	927,806	14,607
1	6.85	0.16	552,951	12,902
2	3.75	0.12	302,491	9700
3	0.52	0.05	41,690	3661
4	0.22	0.03	18,098	2416
5	0.05	0.01	3878	1119
6	0.03	0.01	2585	914
7	0.01	0.01	646	457
8	0.01	0.01	970	560
9	0.01	0.01	646	457

**Table 3.** Estimated annual rate of land-cover change based on binary change/no-change classes derived from LCMAP annual land-cover change product values for all years during 1986–2016, with 1986 “change year” starting on 1 July 1985. The final row gives the total estimated area of gross change over the entire time series.

Year	Change Area of CONUS (%)	SE Change (%)	Change Area (km <sup>2</sup> )	SE Change (km <sup>2</sup> )
1986	0.3020	0.0344	24,374	2776
1987	0.4308	0.0407	34,764	3288
1988	0.6208	0.0488	50,097	3937
1989	0.7251	0.0534	58,518	4308
1990	0.6266	0.0489	50,566	3944
1991	0.6111	0.0488	49,319	3942
1992	0.5551	0.0470	44,796	3792
1993	0.6005	0.0493	48,459	3976
1994	0.5537	0.0463	44,681	3734
1995	0.6005	0.0479	48,463	3868
1996	0.6004	0.0480	48,454	3871
1997	0.5491	0.0462	44,314	3730
1998	0.6490	0.0499	52,376	4028
1999	0.6988	0.0521	56,390	4202
2000	0.7311	0.0535	59,004	4320
2001	0.6282	0.0492	50,693	3972
2002	0.6276	0.0498	50,650	4020
2003	0.6665	0.0509	53,790	4112
2004	0.5871	0.0481	47,380	3885
2005	0.5326	0.0452	42,980	3650
2006	0.5774	0.0475	46,598	3835
2007	0.5322	0.0453	42,952	3659
2008	0.5037	0.0441	40,650	3559
2009	0.4882	0.0433	39,397	3490
2010	0.4935	0.0446	39,827	3595
2011	0.5333	0.0459	43,039	3701
2012	0.6726	0.0517	54,277	4173
2013	0.5211	0.0449	42,050	3620
2014	0.4895	0.0438	39,504	3534
2015	0.4055	0.0399	32,720	3224
2016	0.3249	0.0358	26,221	2888
1986—2016			1,408,393	28,527

The two most prominent patterns of land-cover dynamics were natural resource cycles and increases in urban and built-up land, the latter represented by the developed land-cover class. Natural resource cycles accounted for an estimated  $79.32 \pm 0.85\%$  (Materials and Methods, **ratio of the area of a specific grouping of class change types**) of all annual gross change, with these processes mostly involving the loss and gain of tree cover through harvest, wildfire, other natural events, and its regrowth, as well as fluxes between cropland and grass/shrub. New developed land cover encapsulated more urbanization or built-up land and represented  $10.87 \pm 0.48\%$  of all annual land-cover change. Finally, surface-water dynamics, which affect changes of the water class, comprised  $6.24 \pm 0.68\%$  of all annual change.

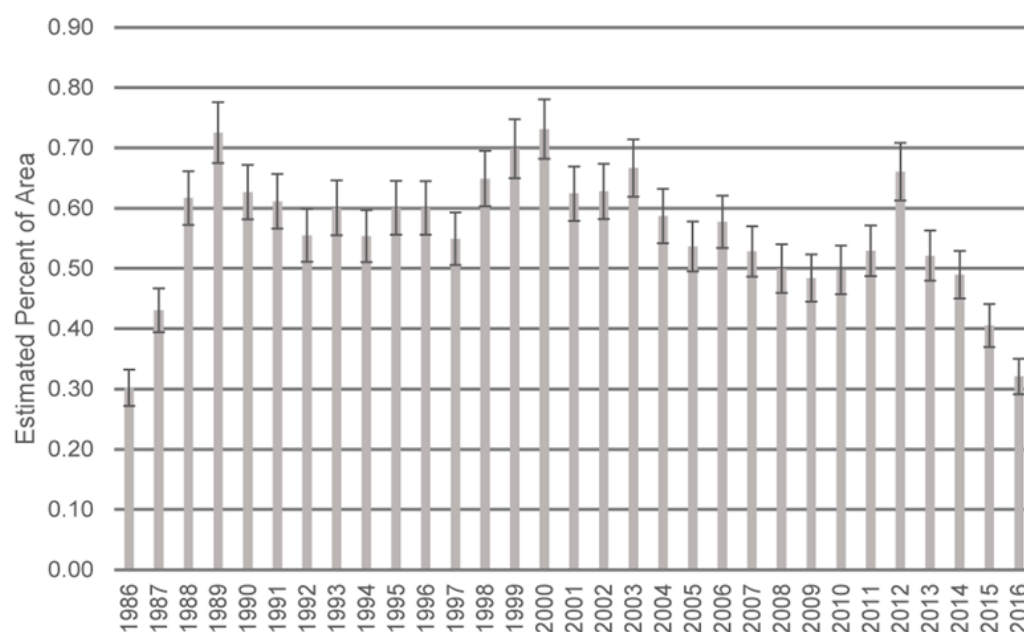


**Figure 1.** Annual estimated percent area of CONUS land-cover class change, 1985–2016 (error bars represent one standard error, 1986 “change year” 1 July 1985 to 30 June 1986).

Specific types of conversion illustrate the importance of understanding net change of a land cover within its overall gross change context. From 1985 to 2016, the estimated net loss in tree cover was  $44,921 \pm 9878 \text{ km}^2$  (Table 1). Cumulative annual gross change in tree cover was dominated by back-and-forth flux between tree cover and grass/shrub. An estimated  $351,613 \pm 11,133 \text{ km}^2$  changed from tree cover to grass/shrub but was offset by a reciprocal change of  $360,662 \pm 11,074 \text{ km}^2$  that changed from grass/shrub to tree cover (Supplementary Dataset S2). A similar flux occurred in cropland with a net decrease of  $109,233 \pm 9485 \text{ km}^2$ . The estimated cumulative annual gross change from cropland to grass/shrub was  $210,063 \pm 8372 \text{ km}^2$ , with much of this amount countered by an estimated  $142,520 \pm 6850 \text{ km}^2$  of the reciprocal change (Supplementary Dataset S2).

Land-cover class change was geographically variable across the CONUS (Figure 2a). At this scale, little land-cover conversion can be seen in the Midwest, Appalachians, Mid-Atlantic, and New England, whereas the southeastern United States, Texas, and coastal Pacific Northwest showed larger cohesive swaths of change. California, other parts of the western United States, much of the Great Plains, and Maine had widespread but dispersed smaller pockets of land-cover change.

### 3.2. Natural Resource Cycles

Natural resource cycles primarily involved changes among three land-cover classes within two different reciprocal changes: (1) tree cover and grass/shrub, and (2) cropland and grass/shrub. The first of these deals primarily with aspects of commercial forestry and loss and recovery from stand-replacing wildfire. These changes, generally exhibiting a cyclic nature between tree cover and grass/shrub, accounted for most of the annual tree cover gross change (Supplementary Dataset S3) (Figure 3a) and represents much of what is seen (purple) in the map of tree-cover change (Figure 2b). Although net change in the area of tree cover was small, there were still single years and series of years where loss outpaced recovery or the reverse were evident (Figure 3a). During the late 1980s tree-cover removal exceeded regrowth, as then record-setting timber volume removal occurred [41], as well as large wildfire events, such as the Yellowstone Park fires of 1988 [42]. The 1990s through approximately 2004 mostly had years where gains in tree cover exceeded losses. The Northwest Forest Plan of 1994 [32] resulted in much less timber removal on public lands of the Pacific Northwest. This helped push the ascendancy of southern U.S. as the

leading industrial forestry region in the nation [43], although its wood production and future trends have been well reported e.g., [44]. Towards the mid-2010s, tree-cover removal again mostly outpaced regrowth (Figure 3a), driven by increasing economic activities after the Great Recession [45], generally larger wildfire years [46] (Figure 4), and in at least one region wildfires during “hotter” droughts [47]. This second era (2012–2016) of net tree-cover loss rivaled the earlier one of the late 1980s and early 1990s.

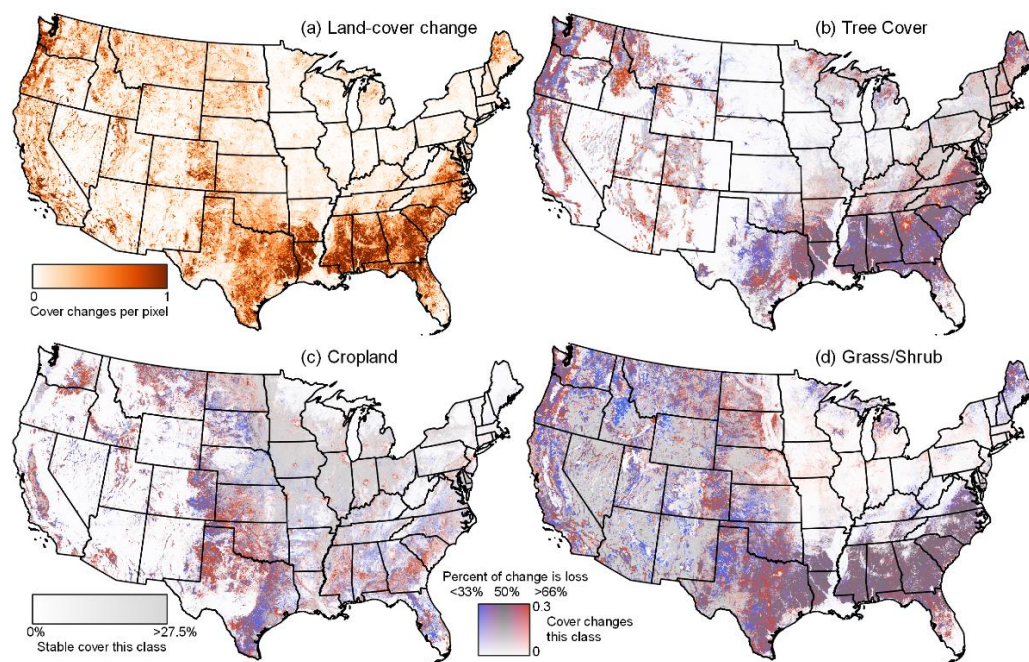


**Figure 2.** Land-cover conversion from 1985 to 2016. Total change is shown in (a) land-cover conversion. In the other three panels, cover change and stable cover are shown for specific classes (b) tree cover, (c) cropland, and (d) grass/shrub. Gray shading shows areas where stable land cover of a specific class is present. Change information is shown by a two-dimensional color scale indicating both the amount and direction of change (blue for gain, red for loss; darker shades for more change). Figure values are derived from a  $3 \times 3$  km ( $100 \times 100$  Landsat pixel) binning of the class change map product (LCACHG, see Section 2).

Natural resource cycles involving reciprocal changes between cropland and grass/shrub can represent new cropland converted from previously never cropped grasslands or shrublands or a return of short-to-longer term idled land to cropland. Interannual climatic conditions, federal policy changes, availability of irrigation water, or other land-use management decisions are some of the reasons for these cycles. These reciprocal class changes make up most of cropland gross change (Figure 3b, Supplementary Dataset S3). During these three decades, more cropland to grass/shrub change occurred than the reverse, corresponding with the initiation, growth, and reduction in area extent of the federal Conservation Reserve Program (CRP) [48]. Reciprocal losses or gains involving cropland generally follow the history of the CRP, with two large growth eras of the program (the late 1980s—with 1989 being the largest single year of enrollment—through 1993, and again, starting in 2000 and ending in 2007) and one major sustained decline in enrollment (from 2008 through 2016) [48,49] (Figure 3b). Other drivers besides CRP were also in play, such as reductions in water allotments for irrigation in some arid regions [50], increased use of groundwater sources in other locations to expand irrigated cropland such as in Nebraska [51], and a ramp-up in biofuel production such as in the Dakotas e.g., [30]—although this may have been in tandem with changes in regional advantage for certain crops [52]. Some of these local-to-regional change stories can be seen in the CONUS map of cropland, along with the stability of non-changing cropland in the Midwest (Figure 2c). Our results

show that cropland declined in area from 1985 to 2016. The U.S. Dept. of Agriculture historical data reinforces that the first half of the 1980s (except during the 1983 Payment in Kind (PIK) program) showed the largest U.S. area under crops in the last 40 years [53,54].

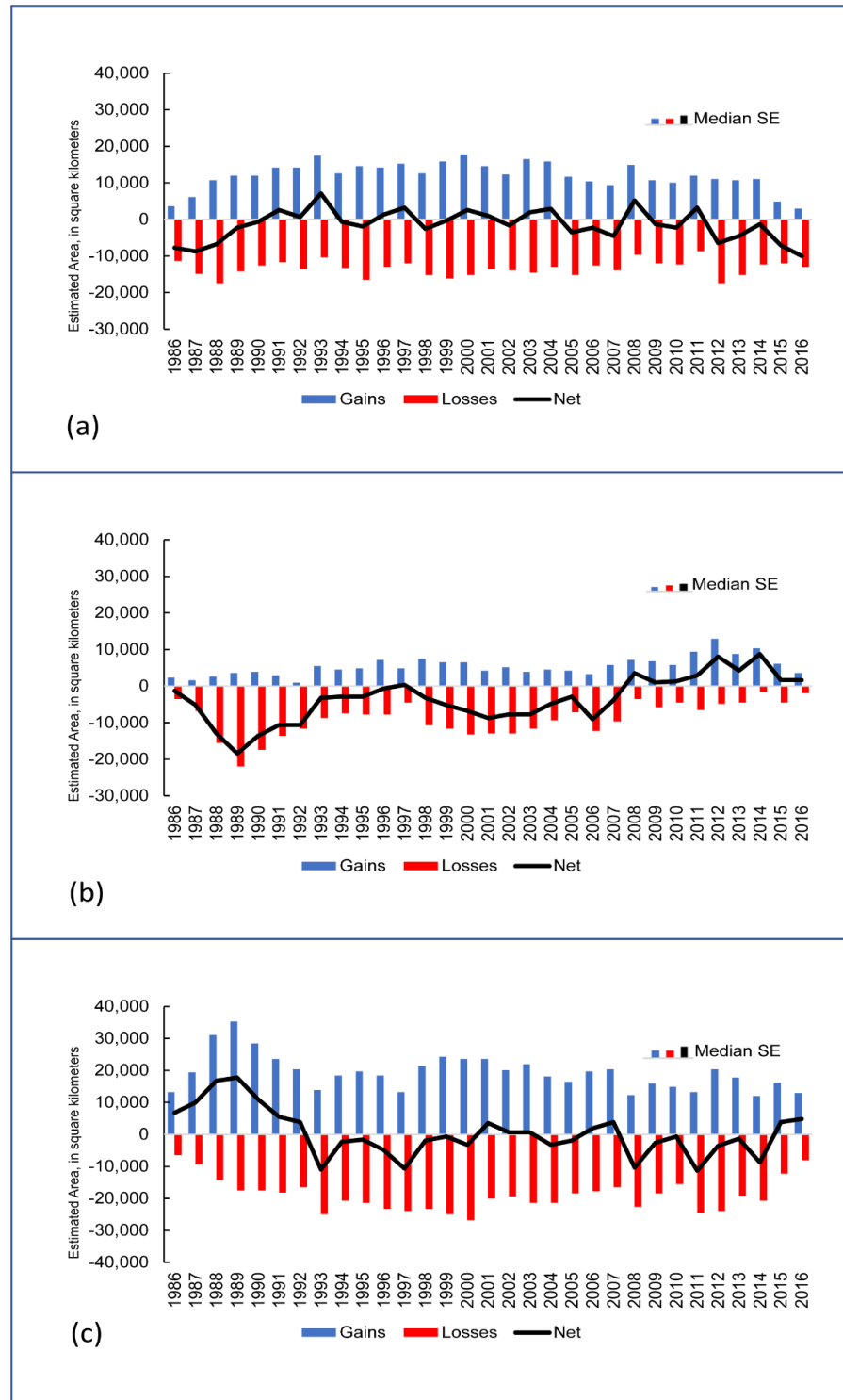


**Figure 3.** Annual gross gains, gross losses, and net change for (a) tree cover, (b) cropland, and (c) grass/shrub, 1985–2016, with 1986 “change year” starting on 1 July 1985). The standard error (SE) inset represents the median of the annual standard errors (in square kilometers) for each estimate: tree cover—gain,  $\pm 1965$ ; loss,  $\pm 2068$ ; and net,  $\pm 2909$ ; cropland—gain,  $\pm 1252$ ; loss,  $\pm 1583$ ; and net,  $\pm 2144$ ; grass/shrub—gain,  $\pm 2501$ ; loss,  $\pm 2501$ ; and net,  $\pm 3540$ .

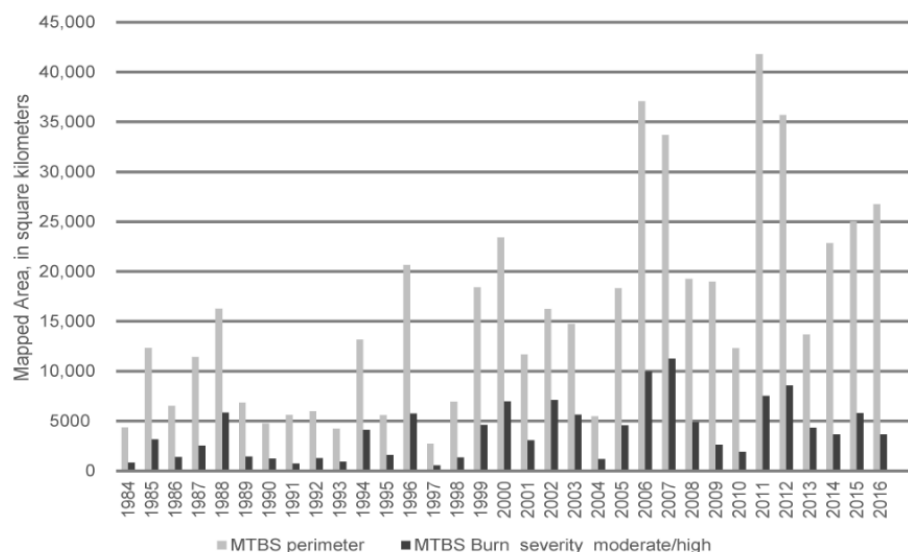


**Figure 4.** Mapped area of major fires and burn severity from Monitoring Trends in Burn Severity map data [46] in the CONUS, 1984–2016.

Grass/shrub not only retained its primary land use for grazing animals in the western CONUS (Figure 2d), but also became the “catch all” repository (e.g., tree cover to grass/shrub, cropland to grass/shrub) for the main types of natural resource-based land-cover class conversions, as seen by the amount of its annual gross change (Figure 3c). These types of changes tended to be transitory, as indicated by grass/shrub in southeastern CONUS where extensive amounts of area show both gain and loss (Figure 2d).

To a smaller extent, two other natural resource cycles that could involve reciprocal land-cover change were associated with mining activities and farming some types of wetlands. Mining, which was included within the developed class, often changed to grass/shrub over time after mining activities ceased, but the cumulative area of mining was small. Wetlands that changed to cropland tended to be cyclic farmable wetlands [55], dry enough to till or hay some years but too wet to grow crops other times. The federal “farm bill” that established CRP in 1985 also included the “Swampbuster” provision that penalized land-use operators from actively draining wetlands [56], thus permanent conversion of wetlands to cropland was limited during the study period, although farming activities in these wetlands may diminish overall ecosystem services and extent over time [57].

### 3.3. Developed Land-Cover Change

Most U.S. residents live in either metropolitan or micropolitan counties [58], and population grew an estimated 35.7% or 85 million people between 1985 and 2016 [59]. During this period, incremental urbanization continued around most cities, although the extent and direction of growth in developed land cover varied. The estimated gain of developed was  $131,209 \pm 6866 \text{ km}^2$  (Table 1), with grass/shrub, tree cover, and cropland providing the main base for this increase (Figures 5a and 6). Grass/shrub conversion to developed often happened around major Sunbelt metropolitan areas (e.g., Figure 5b). Tree cover to developed was found predominantly in the eastern United States (e.g., Figure 5c) and cropland to developed primarily in the Midwest (e.g., Figure 5d).

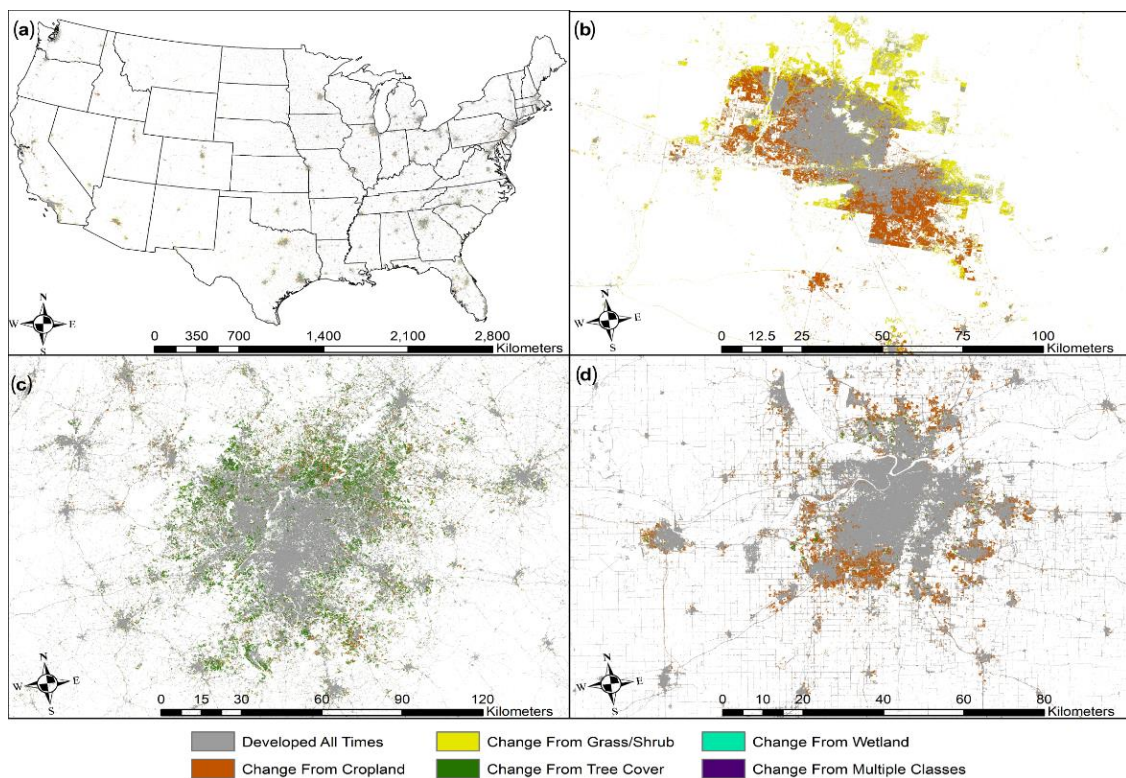


**Figure 5.** Examples of developed land-cover gain within a predominately stable developed land-cover base (a), while new development can be seen at the local scale (b–d). The Phoenix metropolitan area (approximate center coordinate in Decimal Degrees (DD) 33.439081 N, −112.075208 W) is an example of a fast-growing Sunbelt urban area where one of the main sources of new developed land cover was grass/shrub, along with cropland conversion to developed (b). The Atlanta area (approximate center coordinate in DD 33.745106 N, −84.387308 W) is typical of eastern U.S. urban places where tree cover is the primary source of new developed land (c). The Kansas City metropolitan (approximate center coordinate in DD 39.076467 N, −94.602064 W) area’s main source of new developed land cover was from cropland, which is common for Midwest urban areas (d).

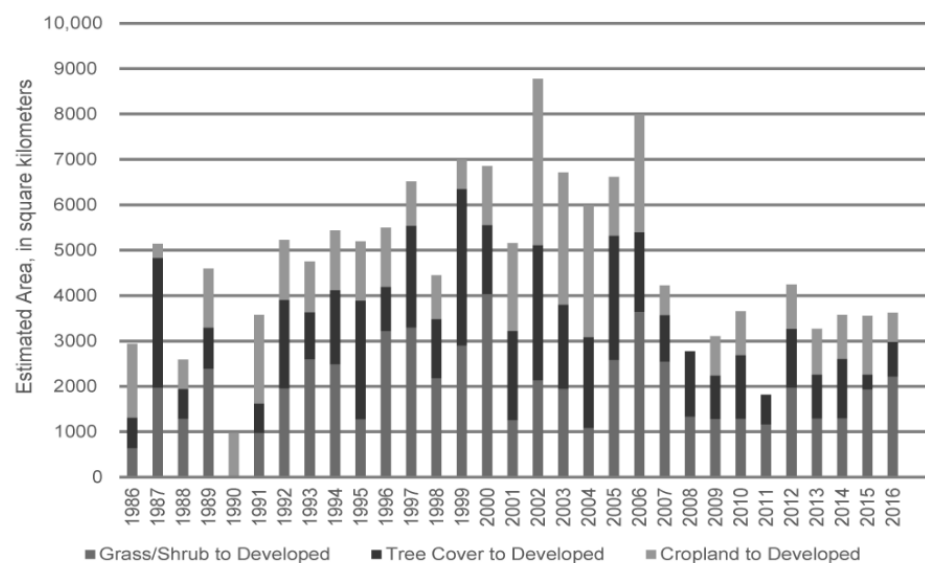


**Figure 6.** Estimated annual area of major sources of change to developed land cover, 1985–2016, with 1986 “change year” starting on 1 July 1985.

The temporal nature of change to developed showed considerable annual variation (Figures 6 and 7a). The early 1990s through 2006 had the greatest area of conversion, and for most years during this period new housing starts exceeded 1.5 million units [60] (Figure 8). New development was greatly affected by the 2007–2008 housing financial crisis and the ensuing Great Recession [60]. This socioeconomic shock appeared to dampen increasing development until late in the study period, but the rate of urbanization did not return to the higher levels that had occurred in the 1990s through 2006. Some evidence also points to a complex generational mix contributing to this lower rate of new development, as the “Millennial” population was more likely residing in the already built environment compared with previous cohorts [61].

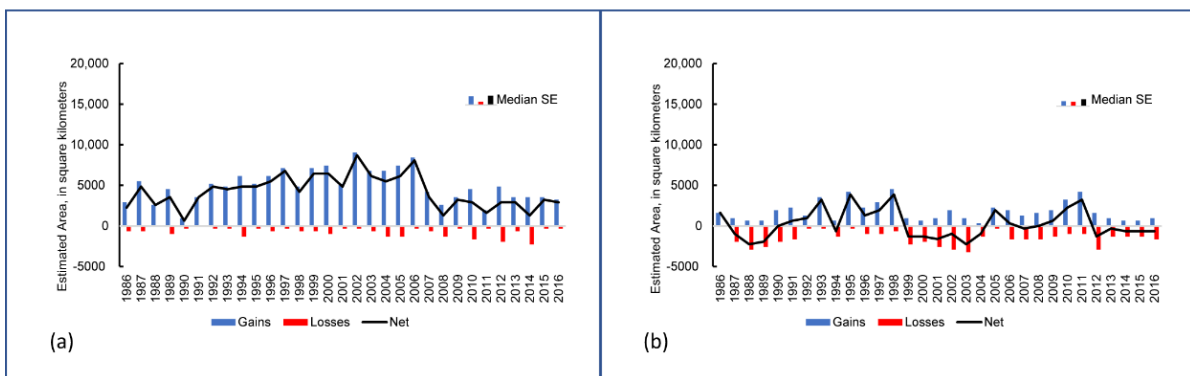


**Figure 7.** Annual gross gains, gross losses, and net change for land-cover classes (a) developed and (b) water. Median standard error (SE) in square kilometers: developed—gain,  $\pm 1252$ ; loss,  $\pm 457$ ; and net,  $\pm 1333$ ; Water—gain,  $\pm 723$ ; loss,  $\pm 646$ ; and net,  $\pm 1022$ .

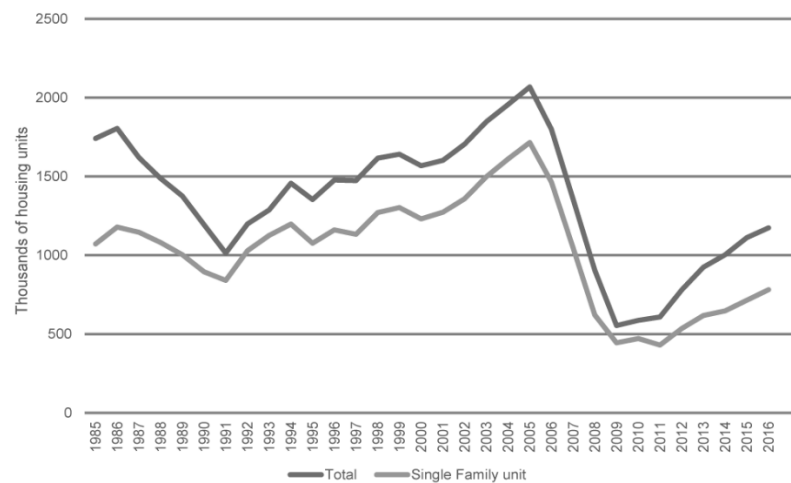


**Figure 8.** U.S. housing unit starts per year [60], 1985–2016.

### 3.4. Surface-Water Dynamics

Surface-water change in the CONUS is also a natural resource with a cyclical dynamic but different from the dynamics observed for tree cover, grass/shrub, and cropland. Water dynamics showed regional differences with areas of expansion and contractions (Figure 9). Although net change in water between 1985 and 2016 was only  $0.10 \pm 0.04\%$ , annual gross change in water was substantial during some years (Figure 7b).

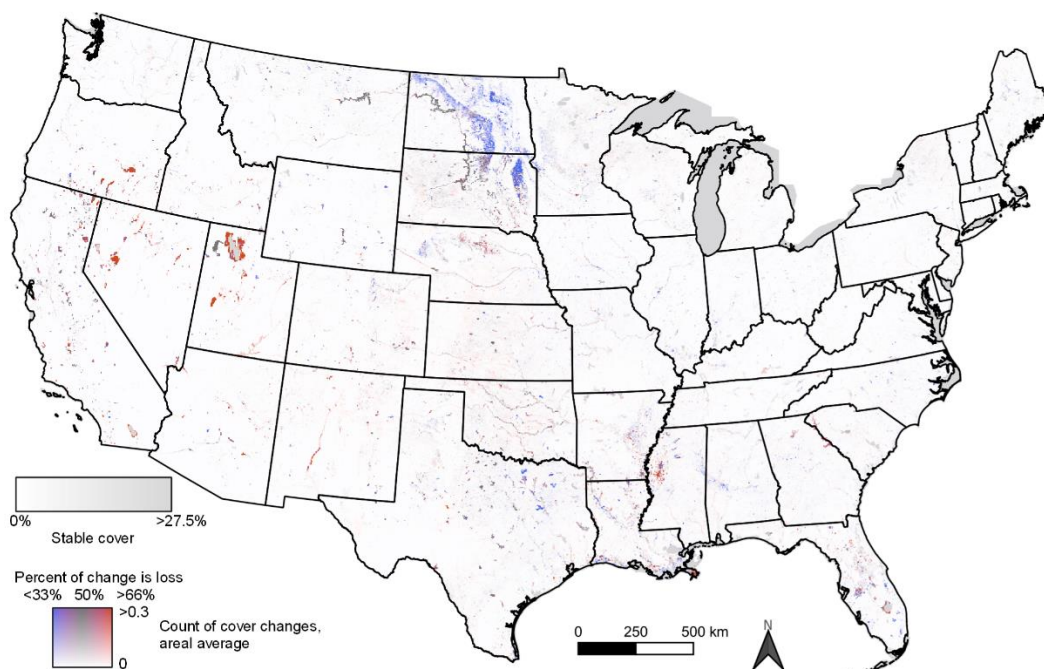


**Figure 9.** Water dynamics during 1985–2016. Gray shading shows areas where stable land cover of a specific class is present. Change information is shown by a two-dimensional color scale indicating both the amount and direction of change (blue for gain, red for loss; darker shades for more change). Figure values are derived from a  $3 \times 3$  km ( $100 \times 100$  Landsat pixel) binning of the class change map product (LCACHG, see Section 2).

The two most noticeable regions of water change were gains in the northern plains of the Dakotas and scattered locations of loss in the Inter-Mountain West. Both areas contain closed hydrologic basins that are heavily dependent on interannual precipitation patterns. Within these areas, different intervals of pluvial and drought years played out. In the northern plains' prairie pothole region, a near-decade-long pluvial era (starting in 1993), the most extreme in nearly a century of record keeping [62], overfilled many of the existing lakes and wetlands, causing increased surface water and localized flooding. Another shorter pluvial interval, centered on 2010, added to or maintained expanded surface water in the region [63]. Both pluvial intervals show up in the overall water annual change as gains in Figure 7b. A pixel-count only differencing from the land-cover maps for water in the Dakotas for the two years of 1985 and 2016 shows almost a 51% increase in 2016.

The Inter-Mountain West closed basins have a complex story but do show the effects of a substantial multi-year drought late in the study period [64], which contributed to the slight net loss of water land cover for the CONUS seen in Figure 7b. The Great Salt Lake of Utah is an example of the greater complexity of regional water change. The beginning of the time series had historically high lake levels in the mid-1980s as a starting point, with the lake returning to more typical levels around the year 2000, which was followed by contraction coming from regional drought and continued high diversion of inflows for nearby anthropogenic land uses [65]. For part of the western CONUS beyond the Inter-Mountain closed basins (all of California, Oregon, Nevada, Utah, and Arizona), a pixel-count only differencing from the land-cover maps for water for the two years of 1985 and 2016 shows nearly a 23% decrease in 2016.

Secondary stories of surface-water change are observed as gains in northeastern Texas and losses in west-central Mississippi. Texas surpassed New York as the second most populated state during the study period [66], and although most of the reservoirs in Texas were built before 1985, several more were added during the study period. The expanding urban complex of metropolitan Dallas and Fort Worth is especially dependent on surface-water impoundments for its needs [67]. The mostly surface-water loss in west-central

Mississippi reflects a boom in the expansion of catfish aquaculture during the late 1980s, where cropland was converted to numerous shallow fishponds followed by an industry-wide decline in the 2000s [68], with ponds being returned to cropland use or being left empty. A sub-region of similar aquaculture expansion was observed in nearby west-central Alabama and into east-central Mississippi.

Other, less prominent clusters of surface-water change, are observed in central and southern Florida, the east and west ends of the Nebraska Sandhills, and scattered across California. Drivers of change were varied across these geographic regions, reinforcing the narrative that no single cause dominated surface-water change during the study period.

#### 4. Discussion and Conclusions

Dominant land-cover class change dynamics in the CONUS between 1985 and 2016 were due to natural resource cycles, with this type of change occurring in an overall footprint of various geographic concentrations. The footprint of tree-cover class change was found primarily in the southern United States, along with parts of northwest CONUS and other, more isolated areas, such as the Inter-Mountain West and western Maine (Figure 2b). The cropland footprint of change was found primarily in the central part of the CONUS, with other areas scattered across the southeast and various smaller concentrations in the west (Figure 2c). Tree cover, cropland, and grass/shrub cycled through forest and agriculture land uses with changes involving grass/shrub often shorter-to-longer term transitory in nature, resulting in most of the footprint of grass/shrub class change seen in Figure 2d. Tree cover experienced years of both net loss and gain, with the loss intervals occurring at the start and end of the study period. Although cropland experienced net gains from 2008 forward, cropland had a net loss at the CONUS scale from 1985 to 2016. Some of this loss could be considered “rotational loss” as land still enrolled in the CRP may return to active cropping at later dates after contracts expire. Both examples illustrate the value of the 30+ year time span monitored by LCMAP.

Most of the developed land cover in the CONUS was already present by 1985 (Figure 5a). However, continued population growth over the study period resulted in substantial conversions to developed coming from different land-cover sources depending on what land was available in specific locations. Rates of “urbanization” by 2016 had not returned to earlier highs that were found in the middle of the study period. Surface-water expansion/contraction also played a role in CONUS change but was generally more diffuse across space and variable in area extent. Water also was influenced by generally different drivers of class change than the other two leading land-cover change groups.

Approximately 88.5% of the CONUS did not experience a land-cover change during the years 1985 through 2016. The geographic footprint of land-cover conversion (11.5% of the area of the CONUS) is composed of greater annual change dynamic because approximately 40% of this area of change experienced more than one land-cover transition over time. Much of this footprint of land-cover conversion was transitory in nature, either early serial stage tree growth represented by LCMAP’s “Grass/Shrub” class or short-to-intermediate length idling of cropland also classified as grass/shrub. How these transitory land-cover areas within a greater spatial context of mostly stable land cover affect human-environmental interactions at multiple scales could be explored in future research. The spread of the footprint of land-cover change and the increasing frequency of the number of conversions occurring on the same land within it could also be explored within the land-dynamics community in the future.

In conclusion, our assessment of the historical changes of land cover that occurred across the CONUS has revealed that relatively small net changes in land-cover classes are not the full reflection of the larger amount of overall gross change that happened. By documenting the annual land-cover change, the gross change, the overall footprint of change, and the frequency of class conversions, we have provided an account of net and gross changes in all land covers. LCMAP’s enhanced temporal-scale monitoring using Landsat data allowed us to dissect a generally stable land-use system across the CONUS,

revealing a complicated change story that we combined with human and environmental drivers to better understand land-cover dynamics.

The broader implication of our work within the land-dynamics community is the emphasis on the temporal nature of change. Leading research topics on forest systems include disturbance and regrowth [35] and changes within the industrial pine plantations in the southeastern United States [43,44]. Similarly, land-cover studies of agricultural regions [9,52], grasslands [26], and developed areas [21] are focused on individual land covers or region. Our study provides context to how individual land covers interplay within the matrix of land covers across the CONUS.

Anticipated future changes associated with climate change [65] highlight the importance of land-change studies. The accounting of net and gross land-cover changes in all landscapes is integral to understanding biodiversity [2], carbon dynamics [6,20], water quality, and natural resource protection [24] in both natural and managed landscapes.

**Supplementary Materials:** The following are available online at <https://www.mdpi.com/article/10.3390/land11020298/s1>, Dataset S1—Annual land cover, 1985–2016, as a percent of the conterminous United States, with standard errors (SE); Dataset S2—Area estimates (square kilometers) of specific land-cover class change across the conterminous United States, cumulative 1985 to 2016, with Standard Errors (SE); Dataset S3—Area estimates (square kilometers) of specific land-cover class change across the conterminous United States, annual 1985 to 2016, with Standard Errors (SE).

**Author Contributions:** Designed research, R.F.A., S.V.S., B.W.P., D.F.W., T.R.L.; performed research, R.F.A., D.F.W., J.L.T., B.W.P., J.A.H., S.V.S., H.J.T.; contributed analytic tools, H.J.T., A.A.M., K.L.S., R.R.R.; analyzed data, R.F.A., J.L.T., D.F.W., S.V.S.; discussed results and wrote the paper, R.F.A., D.F.W., J.L.T., S.V.S., J.F.B., T.R.L., K.L.S., J.A.H., Z.Z., G.X., C.P.B., R.R.R. All authors have read and agreed to the published version of the manuscript.

**Funding:** Funding for this work was provided by the U.S. Geological Survey’s National Land Imagining and Climate Research & Development programs. Work performed by KBR and Innovate! employees was under contract 140G0121D0001.

**Data Availability Statement:** LCMAP Reference Data: U.S. Geological Survey (USGS) Earth Resources Observation and Science (EROS) Center, 2020a, LCMAP Reference Data Product 1984–2018 land cover and land use attributes aggregate data and metadata, <https://doi.org/10.5066/P9ZW0XJ7>. LCMAP Primary Land Cover (LCPRI) and Land Cover Annual Change (LCACHG): U.S. Geological Survey (USGS) Earth Resources Observation and Science (EROS) Center, 2020b, Land Change Monitoring, Assessment, and Projection (LCMAP) Collection 1.0 Science Products, <https://doi.org/10.5066/P9W1TO6E> or <https://earthexplorer.usgs.gov>. LCMAP CONUS Geographic Assessment Data Tables. Auch, R.F.; Wellington, D.F.; Stehman, S.V.; and Taylor, J.F., 2021, LCMAP CONUS Geographic Assessment Data Tables v1.0 1985–2016: U.S. Geological Survey, <https://doi.org/10.5066/P96BM1YV>.

**Acknowledgments:** We would like to acknowledge the help provided by Carol Deering (KBR), librarian of USGS EROS, for multiple literature searches and other bibliographic efforts and Chris Laingen, Eastern Illinois University, for providing reference for USDA historical cropland area estimates. We would also like to thank Mark Drummond, USGS, and three anonymous journal reviewers for helpful comments and suggestions that made this a better article. Any use of trade, firm, or product names is for descriptive purposes and does not imply endorsement by the U.S. Government.

**Conflicts of Interest:** The authors declare no conflict of interest. The funders had no role in the design of the study; in the collection, analyses, or interpretation of data; in the writing of the manuscript, or in the decision to publish the results.

## Appendix A

**Table A1.** LCMAP land-cover class definitions [69].

Land-Cover Class Definition	
Developed	Areas of intensive use with much of the land covered with structures (e.g., high density residential, commercial, industrial, or transportation), or less intensive uses where the land-cover matrix includes vegetation, bare ground, and structures (e.g., low density residential, recreational facilities, cemeteries, transportation/utility corridors), including any land functionally related to the developed or built-up activity.
Cropland	Land in either a vegetated or unvegetated state used in production of food, fiber, and fuels. This includes cultivated and uncultivated croplands, hay lands, orchards, vineyards, and confined livestock operations. Forest plantations are considered as forests or woodlands (Tree Cover class) regardless of the use of the wood products.
Grass/Shrub	Land predominantly covered with shrubs and perennial or annual natural and domesticated grasses (e.g., pasture), forbs, or other forms of herbaceous vegetation. The grass and shrub cover must comprise at least 10% of the area and tree cover is less than 10% of the area.
Tree Cover	Tree-covered land where the tree-cover density is greater than 10%. Cleared or harvested trees (i.e., clearcuts) will be mapped according to current cover (e.g., Barren, Grass/Shrub).
Water	Areas covered with water, such as streams, canals, lakes, reservoirs, bays, or oceans.
Wetland	Where water saturation is the determining factor in soil characteristics, vegetation types, and animal communities. Wetlands are composed of mosaics of water, bare soil, and herbaceous or wooded vegetated cover.
Ice/Snow	Land where accumulated snow and ice does not completely melt during the summer period (i.e., perennial ice/snow).
Barren	Land composed of natural occurrences of soils, sand, or rocks where less than 10% of the area is vegetated.

## References

- Homer, C.; Dewitz, J.; Jin, S.; Xian, G.; Costello, C.; Danielson, P.; Gass, L.; Funk, M.; Wickham, J.; Stehman, S.; et al. Conterminous United States land cover change patterns 2001–2016 from the 2016 National Land Cover Database. *ISPRS J. Photogramm. Remote Sens.* **2020**, *162*, 184–199. [\[CrossRef\]](#)
- Marques, A.; Martins, I.S.; Kastner, T.; Plutzer, C.; Theurl, M.C.; Eisenmenger, N.; Huijbregts, M.A.J.; Wood, R.; Stadler, K.; Bruckner, M.; et al. Increasing impacts of land use on biodiversity and carbon sequestration driven by population and economic growth. *Nat. Ecol. Evol.* **2019**, *3*, 628–637. [\[CrossRef\]](#)
- Loveland, T.R.; Acevedo, W.; Sayler, K.L. Land-Cover Trends in the Eastern United States—1973 to 2000. In *Status and Trends of Land Change in the Eastern United States—1973 to 2000*; Sayler, K.L., Acevedo, W., Taylor, J.L., Auch, R.F., Eds.; US Department of the Interior, US Geological Survey: Washington, DC, USA, 2016; pp. 3–16. [\[CrossRef\]](#)
- McDonald, R.L.; Weber, K.F.; Padowski, J.; Boucher, T.; Shemie, D. Estimating watershed degradation over the last century and its impact on water-treatment costs for the world’s large cities. *Proc. Natl. Acad. Sci. USA* **2016**, *113*, 9117–9122. [\[CrossRef\]](#) [\[PubMed\]](#)
- Modernel, P.; Rossing, W.A.H.; Corbeels, M.; Dogliotti, S.; Picasso, V.; Tittonell, P. Land use change and ecosystem service provision in Pampas and Campos grasslands of southern South America. *Environ. Res. Lett.* **2016**, *11*, 113002. [\[CrossRef\]](#)
- Law, B.E.; Hudiburg, T.W.; Berner, L.T.; Kent, J.J.; Buotte, P.C.; Harmon, M.E. Land use strategies to mitigate climate change in carbon dense temperate forests. *Proc. Natl. Acad. Sci. USA* **2018**, *115*, 3663–3668. [\[CrossRef\]](#)
- Ouyang, Y.; Leininger, T.D.; Moran, M. Impacts of reforestation upon sediment load and water outflow in the Lower Yazoo River watershed, Mississippi. *Ecol. Eng.* **2013**, *61*, 394–406. [\[CrossRef\]](#)
- Hille, S.; Andersen, D.K.; Kronvang, B.; Baattrup-Pedersen, A. Structural and functional characteristics of buffer strip vegetation in an agricultural landscape—High potential for nutrient removal but low potential for plant biodiversity. *Sci. Total Environ.* **2018**, *628–629*, 805–814. [\[CrossRef\]](#)
- Lind, L.; Hasselquist, E.M.; Laudon, H. Towards ecologically functional riparian zones: A meta-analysis to develop guidelines for protecting ecosystem functions and biodiversity in agricultural landscapes. *J. Environ. Manag.* **2019**, *249*, 109391. [\[CrossRef\]](#)

10. Bigelow, D.P.; Borchers, A. *Major Uses of Land in the United States, 2012*; United States Department of Agriculture Economic Research Service: Washington, DC, USA, 2012.
11. Brown, J.F.; Tollerud, H.J.; Barber, C.P.; Zhou, Q.; Dwyer, J.L.; Vogelmann, J.E.; Loveland, T.R.; Woodcock, C.E.; Stehman, S.V.; Zhu, Z.; et al. Lessons learned implementing an operational continuous United States national land change monitoring capability—The Land Change Monitoring, Assessment, and Projection (LCMAP) approach. *Remote Sens. Environ.* **2020**, *238*, 111356. [[CrossRef](#)]
12. Loveland, T.R.; Sohl, T.L.; Stehman, S.V.; Gallant, A.L.; Saylor, K.L.; Napton, D.E. A strategy for estimating the rates of recent United States land-cover changes. *Photogramm. Eng. Remote Sens.* **2002**, *68*, 1091–1099.
13. Estes, J.E.; Loveland, T.R. Toward the use of remote sensing and other data to delineate functional types in terrestrial and aquatic systems. *Dev. Atmos.* **1999**, *24*, 125–150. [[CrossRef](#)]
14. Wulder, M.A.; White, A.C.; Goward, S.N.; Masek, J.G.; Irons, J.R.; Herold, M.; Cohen, W.B.; Loveland, T.R.; Woodcock, C.E. Landsat continuity: Issues and opportunities for land cover monitoring. *Remote Sens. Environ.* **2008**, *112*, 955–969. [[CrossRef](#)]
15. Woodcock, C.E.; Allen, R.; Anderson, M.; Belward, A.; Bindschadler, R.; Cohen, W.; Gao, F.; Goward, S.N.; Helder, D.; Helmer, E.; et al. Free access to Landsat imagery. *Science* **2008**, *320*, 1011. [[CrossRef](#)] [[PubMed](#)]
16. Wulder, M.A.; Masek, J.G.; Cohen, W.B.; Loveland, T.R.; Woodcock, C.E. Opening the archive—How free data has enabled the science and monitoring promise of Landsat. *Remote Sens. Environ.* **2013**, *122*, 2–10. [[CrossRef](#)]
17. Zhu, Z.; Woodcock, C.E. Continuous change detection and classification of land cover using all available Landsat data. *Remote Sens. Environ.* **2014**, *144*, 152–171. [[CrossRef](#)]
18. Zhu, Z.; Gallant, A.L.; Woodcock, C.E.; Pengra, B.; Olofsson, P.; Loveland, T.R.; Jin, S.; Dahal, D.; Yang, L.; Auch, R.F. Optimizing selection of training and auxiliary data for operational land cover classification for the LCMAP initiative. *ISPR J. Photogramm. Remote Sens.* **2016**, *122*, 206–221. [[CrossRef](#)]
19. Chen, L.; Dirmeyer, P.A. Impacts of land-use/land-cover change on afternoon precipitation over North America. *J. Clim.* **2017**, *30*, 2121–2140. [[CrossRef](#)]
20. Liu, J.; Sleeter, B.M.; Zhu, Z.; Loveland, T.R.; Sohl, T.; Howard, S.M.; Key, C.H.; Hawbaker, T.; Liu, S.; Reed, B.; et al. Critical land change information enhances the understanding of carbon balance in the United States. *Glob. Chang. Biol.* **2020**, *26*, 3920–3929. [[CrossRef](#)]
21. Li, C.; Sun, G.; Caldwell, P.V.; Cohen, E.; Fang, Y.; Zhang, Y.; Oudin, L.; Sanchez, G.M.; Meentemeyer, R.K. Impacts of urbanization on watershed water balances across the conterminous United States. *Water Resour. Res.* **2020**, *56*, e2019WR026574. [[CrossRef](#)]
22. Moisen, G.G.; McConville, K.S.; Schroeder, T.A.; Healey, S.P.; Finco, M.V.; Frescino, T.S. Estimating land use and land cover change in north central Georgia: Can remote sensing observations augment traditional forest inventory data? *Forests* **2020**, *11*, 856. [[CrossRef](#)]
23. Rodgers, W.; Mahmood, R.; Leeper, R.; Yan, J. Land cover change, surface mining, and their impacts on a heavy rain event in the Appalachia. *Ann. Am. Assoc. Geogr.* **2018**, *108*, 1187–1209. [[CrossRef](#)]
24. Rittenhouse, C.D.; Pidgeon, A.M.; Albright, T.P.; Culbert, P.D.; Clayton, M.K.; Flater, C.H.; Masek, J.G.; Radeloff, V.C. Land-Cover change and avian diversity in the conterminous United States. *Conserv. Biol.* **2012**, *26*, 821–829. [[CrossRef](#)] [[PubMed](#)]
25. Hansen, M.C.; Egorov, A.; Potapov, P.V.; Stehman, S.V.; Tyukavina, A.; Turubanova, S.A.; Roy, D.P.; Goetz, S.J.; Loveland, T.R.; Ju, J.; et al. Monitoring conterminous United States (CONUS) land cover change with Web-Enabled Landsat Data (WELD). *Remote Sens. Environ.* **2014**, *140*, 466–484. [[CrossRef](#)]
26. Wright, C.K.; Wimberly, M.C. Recent land use change in the Western Corn Belt threatens grasslands and wetlands. *Proc. Natl. Acad. Sci. USA* **2013**, *110*, 4134–4139. [[CrossRef](#)] [[PubMed](#)]
27. Gong, P.; Li, X.; Wang, J.; Bai, Y.; Chen, B.; Hu, T.; Liu, X.; Xu, B.; Yang, J.; Zhang, W.; et al. Annual maps of global artificial imperious area (GAIA) between 1985 and 2018. *Remote Sens. Environ.* **2020**, *236*, 111510. [[CrossRef](#)]
28. Li, Y.; Zhou, Y.; Zhu, Z.; Cao, W. A national dataset of 30 m annual urban extent dynamics (1985–2015) in the conterminous United States. *Earth Syst. Sci. Data* **2020**, *12*, 357–371. [[CrossRef](#)]
29. US Department of Agriculture. *Summary Report: 2017 National Resources Inventory, Natural Resources Conservation Service, Washington, DC, and Center for Survey Statistics and Methodology*; Iowa State University: Ames, IA, USA, 2020. Available online: <https://www.nrcs.usda.gov/wps/portal/nrcs/main/national/technical/nra/nri/results/> (accessed on 10 September 2021).
30. Lark, T.J.; Salmon, J.M.; Gibbs, H.K. Cropland expansion outpaces agricultural and biofuel policies in the United States. *Environ. Res. Lett.* **2015**, *10*, 044003. [[CrossRef](#)]
31. Radwan, T.M.; Blackburn, G.A.; Whyatt, J.D.; Atkinson, P.M. Global land cover trajectories and transitions. *Sci. Rep.* **2021**, *11*, 12814. [[CrossRef](#)]
32. Sleeter, B.M.; Sohl, T.L.; Loveland, T.R.; Auch, R.F.; Acevedo, W.; Drummond, M.A.; Saylor, K.L.; Stehman, S.V. Land-Cover change in the conterminous United States from 1973 to 2000. *Glob. Environ. Chang.* **2013**, *23*, 733–748. [[CrossRef](#)]
33. Pontius, R.G., Jr.; Krithivasan, R.; Sauls, L.; Yan, Y.; Zhang, Y. Methods to summarize change among land categories across time intervals. *J. Land Use Sci.* **2017**, *12*, 218–230. [[CrossRef](#)]
34. Pengra, B.W.; Stehman, S.V.; Horton, J.A.; Dockter, D.J.; Schroeder, T.A.; Yang, Z.; Cohen, W.B.; Healey, S.P.; Loveland, T.R. Quality control and assessment of interpreter consistency of annual land cover reference data in an operational national monitoring program. *Remote Sens. Environ.* **2020**, *238*, 111261. [[CrossRef](#)]
35. Cohen, W.B.; Yang, Z.; Kennedy, R. Detecting trends in forest disturbance and recovery using yearly Landsat time series: 2. TimeSync—Tools for calibration and validation. *Remote Sens. Environ.* **2010**, *114*, 2911–2924. [[CrossRef](#)]

36. Pengra, B.W.; Stehman, S.V.; Horton, J.A.; Wellington, D.F. LCMAP Collection 1 Annual Land Cover and Land Cover Change Validation Tables. *U.S. Geol. Surv. Data Release* **2020**. [CrossRef]
37. Stehman, S.V.; Pengra, B.W.; Horton, J.A.; Wellington, D.F. Validation of the U.S. Geological Survey's Land Change Monitoring, Assessment and Projection (LCMAP) collection 1.0 annual land cover products 1985–2017. *Remote Sens. Environ.* **2021**, *265*, 112646. [CrossRef]
38. Olofsson, P.; Foody, G.M.; Herold, M.; Stehman, S.V.; Woodcock, C.E.; Wulder, M.A. Good practices for estimating area and assessing accuracy of land change. *Remote Sens. Environ.* **2014**, *148*, 42–57. [CrossRef]
39. Cochran, W.G. *Sampling Techniques*, 3rd ed.; Wiley: New York, NY, USA, 1977; p. 413.
40. Stehman, S.V. Estimating area from an accuracy assessment error matrix. *Remote Sens. Environ.* **2013**, *132*, 202–211. [CrossRef]
41. Oswalt, S.N.; Smith, W.B.; Miles, P.D.; Pugh, S.A. Forest Resources of the United States, 2017: A technical document supporting the Forest Service 2020 RPA Assessment. *USDA USFS Gen. Tech. Rep.* **2019**, *97*, 223. [CrossRef]
42. Wright Parmenter, A.; Hansen, A.; Kennedy, R.E.; Cohen, W.; Langner, U.; Lawrence, R.; Maxwell, B.; Gallant, A.; Aspinall, R. Land use and land cover change in the greater Yellowstone ecosystem: 1975–1995. *Ecol. Appl.* **2003**, *13*, 687–703. [CrossRef]
43. Cox, T.R. *The Lumberman's Frontier: Three Centuries of Land Use, Society, and Change in America's Forests*; Oregon State University Press: Corvallis, OR, USA, 2010; p. 510.
44. Wear, D.N.; Greis, J.G. (Eds.) *The Southern Forest Futures Project: Technical Report*; Gen. Tech. Rep. SRS-GTR-178; United States Department of Agriculture, Forest Service, Southern Research Station: Asheville, NC, USA, 2013; 542p. [CrossRef]
45. Berg, E.; Morgan, T.; Simmons, E. *Timber Products Output (TPO)—Forest Inventory, Timber Harvest, Mill and Logging Residue—Essential Feedstock Information Needed to Characterize the NARA Supply Chain, Final Report*; Northwest Advanced Renewables Alliance; Washington State University: Pullman, WA, USA, 2016; Available online: <http://www.bber.umt.edu/pubs/forest/biomass/NARATimberProdOutputfinal.pdf> (accessed on 17 November 2020).
46. USGS; USFS. Burned Area Boundaries Dataset 1984–2017. Monitoring Trends in Burn Severity. Available online: <https://mtbs.gov/direct-download> (accessed on 13 April 2020).
47. Dwomoh, F.K.; Brown, J.F.; Tollerud, H.J.; Auch, R.F. Hotter drought escalates tree cover declines in blue oak woodlands of California. *Front. Clim.* **2021**, *3*, 689945. [CrossRef]
48. Laingen, C.R. A geo-temporal analysis of the conservation reserve program: Net vs. gross change, 1986–2013. *Pap. Appl. Geogr.* **2013**, *36*, 37–46.
49. USDA; FSA. CRP Enrollment and Rental Payment by State, 1986–2018 (xls). Available online: <https://www.fsa.usda.gov/programs-and-services/conservation-programs/reports-and-statistics/conservation-reserve-program-statistics/index> (accessed on 13 April 2020).
50. Soular, C.E.; Wilson, T.S. Recent land-use/land-cover change in the central California Valley. *J. Land Use Sci.* **2015**, *10*, 59–80. [CrossRef]
51. Brown, J.F.; Pervez, M.S. Merging remote sensing data and national agricultural statistics to model change in irrigated agriculture. *Agric. Syst.* **2014**, *127*, 28–40. [CrossRef]
52. Auch, R.F.; Xian, G.; Laingen, C.R.; Saylor, K.L.; Reker, R.R. Human drivers, biophysical changes, and climatic variation affecting contemporary cropping proportions in the northern prairie of the U.S. *J. Land Use Sci.* **2018**, *13*, 32–58. [CrossRef]
53. USDA; ERS. Major Land Uses, Summary Table 3: Cropland Used for Crops: Cropland Harvested (including Double-Cropped), Crop Failure, and Cultivated Summer Fallow for the United States, Annual, 1910–2019. Available online: [https://www.ers.usda.gov/webdocs/DataFiles/52096/Summary\\_Table\\_1\\_major\\_uses\\_of\\_land\\_by\\_region\\_and\\_state\\_2012.xls?v=0](https://www.ers.usda.gov/webdocs/DataFiles/52096/Summary_Table_1_major_uses_of_land_by_region_and_state_2012.xls?v=0) (accessed on 28 September 2021).
54. USGAO. 1983 Payment-in-Kind Program Overview: Its Design, Impact, and Cost; RCED-85-89. 1985. Available online: <https://www.gao.gov/products/rced-85-89> (accessed on 28 September 2021).
55. USDA; FSA. Farmable Wetlands Program. Available online: <https://www.fsa.usda.gov/programs-and-services/conservation-programs/farmable-wetlands/index> (accessed on 14 April 2020).
56. USDA; NRCS. Wetland Conservation Provisions (Swampbuster). Available online: <https://www.nrcs.usda.gov/wps/portal/nrcs/detailfull/national/programs/alphabetical/camr/?cid=stelprdb1043554>. (accessed on 14 April 2020).
57. Verhoeven, J.T.A.; Setter, T.L. Agricultural use of wetlands: Opportunities and limitations. *Ann. Bot.* **2010**, *105*, 155–163. [CrossRef]
58. USCB. Map-U.S. Metropolitan and Micropolitan Counties. 2017. Available online: [https://www2.census.gov/geo/maps/metroarea/us\\_wall/Aug2017/cbsa\\_us\\_0817.pdf?#](https://www2.census.gov/geo/maps/metroarea/us_wall/Aug2017/cbsa_us_0817.pdf?#) (accessed on 14 April 2020).
59. USCB. U.S. Population by Year, July 1 Estimates. Available online: <https://www.multpl.com/united-states-population/table/by-year> (accessed on 14 April 2020).
60. USCB. New Residential Construction, Historical Data, Housing Unit Started (xls). Available online: [https://www.census.gov/construction/nrc/historical\\_data/index.html](https://www.census.gov/construction/nrc/historical_data/index.html) (accessed on 14 April 2020).
61. Lee, H. Are millennials coming to town? Residential location choice of young adults. *Urban Aff. Rev.* **2020**, *56*, 564–604. [CrossRef]
62. Liu, G.; Schwartz, F.W. An integrated observational and model-based analysis of the hydrologic response of prairie pothole systems to variability in climate. *Water Resour. Res.* **2011**, *47*, W02504. [CrossRef]
63. Todhunter, P.E. A volumetric water budget of Devils Lake (USA): Non-Stationary precipitation–runoff relationships in an amplifier terminal lake. *Hydrol. Sci. J.* **2018**, *63*, 1275–1291. [CrossRef]

64. Svoboda, M.; LeComte, D.; Hayes, M.; Heim, R.; Gleason, K.; Angel, J.; Rippey, B.; Tinker, R.; Palecki, M.; Stooksbury, D.; et al. The Drought Monitor. *Bull. Am. Meteorol. Soc.* **2002**, *83*, 1181–1190. [[CrossRef](#)]
65. Baxter, B.K.; Butler, J.K. Climate Change and Great Salt Lake. In *Great Salt Lake Biology*; Baxter, B.K., Butler, J.K., Eds.; Springer: Cham, Switzerland, 2020; pp. 23–52. [[CrossRef](#)]
66. Roberts, S. *A Rank that Rankles: New York Slips to No. 3; Now Texas is 2nd Most Populous State*; The New York Times: New York, NY, USA, 19 May 1994; Section B; p. 1.
67. Gooch, T.; Albright, J.; Ickert, R.A. Water availability modeling for regional water planning. In *Texas in World Environmental and Water Resources Congress 2011—Bearing Knowledge for Sustainability Proceedings*; Beighley, E.R., Killgore, M.W., Eds.; American Society of Civil Engineers: New York, NY, USA, 2011; pp. 2987–2996. [[CrossRef](#)]
68. Kumar, G.; Engle, C.; Hegde, S.; van Senten, J. Economics of U.S. catfish farming practices: Profitability, economies of size, and liquidity. *J. World Aquac. Soc.* **2020**, *51*, 829–846. [[CrossRef](#)]
69. USGS. Land Change Monitoring, Assessment, and Projection (LCMAP Data Format Control Book (DFCB): U.S. Geological Survey, LSDS 1424. 2020. Available online: <https://www.usgs.gov/media/files/lcmap-dfcb> (accessed on 15 December 2021).